Core−Shell Latex Particles Containing a Fluorinated Polymer in the Shell. 2. Internal Structure Studied by Fluorescence Nonradiative Energy Transfer

Pierre Marion,[†] Gérard Beinert,[†] Didier Juhué,[‡] and Jacques Lang*,[†]

Institut Charles Sadron (CRM-EAHP), CNRS-ULP Strasbourg, 6, rue Boussingault, 67083 Strasbourg Cédex, France, and ELF-Atochem, CERDATO, LEM, 27470 Serquigny, France

Received March 14, 1996; Revised Manuscript Received September 13, 1996[⊗]

ABSTRACT: The internal structure of core−shell latex particles, containing a fluoropolymer in the shell, was determined by the fluorescence nonradiative direct energy transfer (NRET) technique. Contrast was achieved by labeling the core and the shell with fluorescent dyes, a donor and an acceptor, respectively and inversely. Donor fluorescence emission intensity was recorded in dilute latex dispersions. Analysis of donor fluorescence decay was carried out by choosing a donor concentration profile within the particles. The analysis revealed the absence of a sharp boundary between the core and the shell, but rather a diffuse interface, which was quantified to within a few tens of nanometers for our ca. 230 nm diameter particles. The scale of this interface was changed by varying the compatibility between the core and the shell.

I. Introduction

Characterization of the internal structure of core−shell latex particles is an outstanding problem of considerable importance with direct relevance for applications in the chemical, biological, and pharmaceutical industries. There is therefore a need for techniques that provide information on the distribution of the polymers which form the core and the shell of the particle.

Previous works have shown that the synthesis of core−shell latex particles is not straightforward and that success depends on many factors, such as the synthesis (batch, stage polymerization, semicontinuous) or the degree of incompatibility between the polymers which form the core and the shell of the particles. Other parameters can influence the internal structure of core−shell particles such as the relative interfacial tension between the two polymers and between each polymer and the water phase, or the rate of transport and the solubility of monomers, oligomers, and radicals in water. Although a rationalization of the morphology of composite particles has been suggested by Sundberg and collaborators,[1] prediction of the morphology of core−shell particles is still not possible and therefore many methods are employed to probe the detailed internal structure of core−shell latex particles. Among the methods most often used is transmission electron microscopy (TEM), which was one of the first methods employed for this purpose in the early seventies.[2−4] TEM has been used for many subsequent structural studies of core−shell latex particles.[5−12] Other methods such as small angle neutron[11,13,14] or X-ray[15−17] scattering, high-resolution NMR,[18] or titration methods[19,20] have also been used. Dynamic mechanical spectroscopy[21−23] and atomic force microscopy[24] were also employed to show evidence of core−shell morphology. Recently, fluorescence nonradiative energy transfer (NRET) has been used to investigate the internal structure of core−shell particles.[25,26]

In this article we describe the synthesis of core−shell latex particles whose cores are formed of poly(butyl methacrylate) (PBMA), with shells comprised of poly(butyl methacrylate-*co*-butyl acrylate-*co*-trifluoroethyl methacrylate) (PBBT), and we examine the internal structure of these particles by means of NRET. For the analysis of the data we use a simple concentration gradient model for the distribution of the donor- and acceptor-labeled polymer chains inside the particles.

II. Experimental Section

A. Materials. Butyl acrylate (BA) and trifluoroethyl methacrylate (TFEM) were obtained from Atochem, styrene (St) is a gift from the EAHP (Strasbourg), butyl methacrylate (BMA) and potassium persulfate (KPS) were purchased from Aldrich, sodium hydrogen carbonate ($NaHCO_3$) is from Prolabo, allyl methacrylate (AMA, cross-linking agent) and azobis(isobutyronitrile) (AIBN) are from Fluka, and sodium dodecyl sulfate (SDS) is from Touzard and Matignon. SDS was recrystallized three times from mixtures of water and ethanol. All other compounds were of the best grade available. The donor, (9-phenanthryl)methyl methacrylate (PheMMA), and the acceptor, 9-anthryl methacrylate (AnMA), were synthesized following the recipe given elsewhere.[27] Water was freshly deionized and distilled before use.

B. Latex Synthesis. The latex particles were synthesized by semicontinuous free radical emulsion polymerization using potassium persulfate as initiator and following a procedure described by Zhao et al.[27] First a latex seed was prepared and next the rest of the components were slowly added in two steps. In each of the slow steps, the aqueous phase (containing the KPS and the SDS) and the organic phase (the monomers) were added separately to the reactor. The polymerization temperature was 80 °C. The slow steps were performed over about 5 h each, next the dispersion was left at 80 °C, gently stirring, for an additional 10 h. The donor (acceptor) was added with the monomers during the first slow step following the seed, and the acceptor (donor) during the second slow step. This second step was started 1 h after the end of the addition of the components of the first step, to allow the consumption of all the monomer of the core before starting to feed the shell monomers. During this period of time, the emulsion was maintained at a temperature of 80 °C. The molar concentration ratio [donor or acceptor]/[monomers] was 0.01.

The latex particles were synthesized from BA, BMA, and TFEM monomers. The recipes and polymerization conditions are given in Table 1. The main characteristics of the latexes

* To whom correspondence should be addressed.
† Institut Charles Sadron.
‡ ELF-Atochem.
⊗ Abstract published in *Advance ACS Abstracts,* December 15, 1996.

S0024-9297(96)00392-0 CCC: $14.00

Table 1. Recipes and Polymerization Conditions for the Core−Shell (CS1 to CS9) Latex Synthesis

step	composition (g)	CS1	CS2	CS3	CS4	CS5	CS6	CS7	CS8	CS9
seed (batch)	water	45.05	45.11	44.93	45.08	45.15	45.07	44.88	45.18	45.02
(80 °C)	KPS	0.0425	0.0419	0.0428	0.0417	0.0422	0.0427	0.043	0.0421	0.0426
	SDS	0.0302	0.0305	0.031	0.0316	0.0311	0.0304	0.0309	0.0303	0.0313
	$NaHCO_3$	0.082	0.081	0.082	0.08	0.081	0.082	0.082	0.08	0.082
	BMA	2.92	2.915	2.93	2.93	2.925	2.91	2.92	2.935	2.92
first slow	water	14.05	13.95	10.1	9.9	10	10.2	10.1	10	13.9
step (5h)	KPS	0.025	0.024	0.018	0.0176		0.0182	0.0179	0.018	0.025
(80 °C)	AIBN					0.05				
	SDS	0.241	0.237	0.139	0.141	0.14	0.138	0.14	0.07	0.08
	BMA	15.73	15.7	11.54	11.55	11.53	11.56	11.52	6.24	10.84
	AMA						0.58			
	BA								1.85	1.72
	styrene								3.47	3.14
	PheMMA		0.305		0.224					
	AnMA	0.289		0.213		0.212	0.214	0.213	0.213	0.288
second slow	water	6.05	6	10.1	10.15	9.95	10.05	10.1	10	5.95
step (5h)	KPS	0.0105	0.011	0.0175	0.018	0.0183	0.0177	0.018	0.0178	0.0181
(80 °C)	SDS	0.08	0.081	0.137	0.0141	0.0139	0.014	0.0142	0.0142	0.04
	BMA	1.28	1.275	2.192	2.185		2.191			
	BA	1.42	1.41	2.4	2.41	3.11	2.41		3.12	1.82
	TFEM	4.04	4.05	6.92	6.93	8.43	6.93	11.55	8.42	4.92
	PheMMA	0.122		0.223		0.206	0.205	0.204	0.206	0.122
	AnMA		0.115		0.198					

Table 2. Symbols Used in the Text, Composition of the Particles and Diameter Measured by AFM, and Theoretical Core Radius and Shell Thickness, for the Synthesized Latex Particles (Phe = Phenanthrene-Labeled Polymer Chains and An = Anthracene-Labeled Polymer Chains)

					theoretical	
	core−shell theoretical	chemical composition		measd particle	core radius[a]	shell thickness[b]
latex	structure (wt %)	core	shell	diam (nm)	(nm)	(nm)
CS1	74−26	PBMA(An)	PBBT1(Phe)	250	113	12
CS2	74−26	PBMA(Phe)	PBBT1(An)	260	118	12
CS3	56−44	PBMA(An)	PBBT1(Phe)	272	112	24
CS4	56−44	PBMA(Phe)	PBBT1(An)	260	107	23
CS5	56−44	PBMA(An) AIBN	PBBT2(Phe)	360	148	32
CS6	56−44	PBMA(An) AMA 5 wt %	PBBT2(Phe)	232	96	20
CS7	56−44	PBMA(An)	PTFEM(Phe)	274	113	24
CS8	56−44	P(BMA−BA−St)(An) 54−16−30 wt %	PBBT2(Phe)	290	119	26
CS9	74−26	P(BMA−BA−St)(An) 69−11−20 wt %	PBBT2(Phe)	284	128	14

[a] Calculated from the measured particle diameter and the quantity of core polymer introduced during the synthesis. [b] Calculated from the measured particle diameter and the quantity of shell polymer introduced during the synthesis.

are reported in Table 2. In most cases the core of the composite particles was made of pure PBMA and the shell of the statistical copolymer PBBT (poly(butyl methacrylate-*co*-butyl acrylate-*co*-trifluoroethyl methacrylate)). The composition of the shell was chosen in such a way that its T_g matches the T_g of the core, equal to 34 ± 3 °C. Two different copolymers for the shell were used, called PBBT1 and PBBT2 in Table 2. The composition of the PBBT1 was 60, 21, and 19 wt % of TFEM, BA, and BMA, respectively (latex CS1 to CS4), and the composition of the PBBT2 was 73 and 27 wt % of TFEM and BA, respectively (latex CS5, CS6, CS8, and CS9). This latter copolymer was richer in fluorinated monomer than the first one. In the case of CS8 and CS9 the core was made of a copolymer containing styrene with the addition of butyl acrylate in order to maintain its T_g at 34 °C.

Modifications to the above procedure were made in some cases. For latex CS5, AIBN was used as initiator for the synthesis of the core of the particles, and for latex CS6, a small quantity (5 wt %) of the cross-linking agent, allyl methacrylate, was added during the synthesis of the core. The shell of the latex CS7 is made of pure poly(trifluoroethyl methacrylate) (PTFEM, T_g = 80 °C). In this case the T_g of the shell is different from the T_g of the core.

Each latex synthesized for this study carries a different label in the core and in the shell. The donor is located in the shell and the acceptor is in the core for CS1, CS3, and CS5 to CS9, and inversely for CS2 and CS4. These labelings are schematically shown in Figure 1. Proper labeling of the polymer chains was checked using a UV detector coupled to a GPC apparatus.

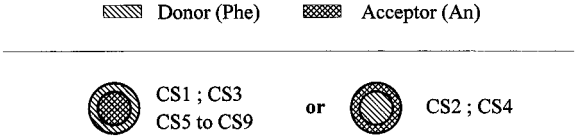

Figure 1. Schematic representation of the labeling of the various core−shell particles synthesized.

C. Latex Particle Size Measurements. Films were prepared by casting 2−3 drops of dispersion (25 wt % solid content) onto freshly cleaved mica plates and allowing these to air dry. Particle diameters were determined on latex dry films by atomic force microscopy (AFM) from the particles height profile using the AFM software, as shown in Figure 2. The AFM was working in the height mode, which means that the force exerted on the film by the cantilever during scanning was kept constant. The model used was a Nanoscope III from Digital Instruments, Inc., Santa Barbara, CA. The spring constant of the cantilever was 0.58 $N \cdot m^{-1}$. The diameters of the particles synthesized in this work are given in Table 2. Besides the determination of the size of the particles, AFM allowed an evaluation of the shape and the polydispersity of the particles. It also allowed following in an easy way the evolution of the size,[26,28] and thus of the number of particles in the course of the latex synthesis. AFM images revealed

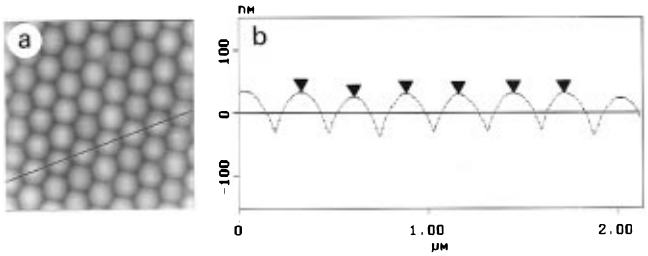

Figure 2. AFM top view (a) (size: 2 μm × 2 μm) and height profile (b) of CS3 latex film. The height profile is taken along the line shown on the top view image. The diameter of the particles (272 nm) is obtained from the average distance between two adjacent triangles, which indicate particle centers, using the AFM software. For each latex studied, at least 30 values have been measured to obtain the average diameter given in Table 2 for the various core−shell particles.

that all particles investigated in this study had a spherical shape and a very low size polydispersity (see Figure 2a) and that no second nucleation had occurred. Indeed, it was important to check that no second nucleation had occurred during the synthesis, and in particular during the synthesis of the shell, and that the particles were spherical in shape, rather than half-moon shaped for instance, since otherwise the interpretation of the fluorescence data, which is based on spherical core−shell particles, would have been meaningless.

D. Latex Particles for Energy Transfer Measurements. The study of the internal core−shell structure of the particles presented in this paper was carried out with latex particles dispersed in water at a very low concentration, about 0.2 wt %. Thus, there was a very low probability for energy transfer between particles. Therefore, the NRET results reported here concern isolated particles only.

E. Fluorescence Decay Measurements. Phenanthrene fluorescence decay traces were recorded with a single photon counting apparatus.[29] Latex dispersions, placed in a squared cell, were excited at 298 nm. The emission light was collected through a band pass filter (Schott) centered at 366 nm to minimize the uptake of scattered and acceptor (anthracene) emitted light. All measurements were performed at 10 °C, i.e. below the T_g of the polymers, to avoid any kind of evolution in the particles during the illumination time.

III. Analysis of the Fluorescence Decay Curves from Latex Dispersion and Modeling of the Particle Core−Shell Interface

A. Analysis of the Fluorescence Decay Curves from Latex Dispersions. As will be seen, our analysis of the donor fluorescence decay is based on a distribution profile of the donor- and acceptor-labeled polymer chains inside the particles. However, for comparison we have also used the simplified model proposed by Winnik and collaborators[27,30−35] which assumes that the donor intensity decay is due to two distinct regions, one region where the donor-labeled polymer chains are far away from any acceptor-labeled polymer chain, and another region where the donor- and acceptor-labeled polymer chains are mixed. Only in this latter region does energy transfer occur. This model has been found very useful for the study of polymer chain migration between adjacent particles in latex films.[25−28,30−41] It has already been transposed to interpret energy transfer occurring inside latex particles,[25,26] where the core polymer was labeled with the donor and the shell-polymer with the acceptor, as shown in Figure 3. Using this model, the interpretation of the donor intensity decay is derived from the Förster equation[42] of NRET and based on the fact that the donors and the acceptors are static during the fluorescence measurements. The energy transfer depends only on the average donor−acceptor distance

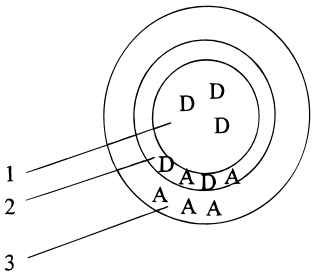

Figure 3. Schematic representation of the simplified model with two uniform concentrations for the donors (D), and for the acceptors (A), inside a latex particle. Regions 1 and 3 contain only donor- and acceptor-labeled polymer chains, respectively. Region 2 contains a mixture of donor- and acceptor-labeled polymer chains. The donor fluorescence intensity comes from regions 1 (second term in eq 1) and 2 (first term in eq 1).

in the range 0−50 Å, for the couple phenanthrene−anthracene used in this work, which is small compared to the particles size (see Table 2). The donor fluorescence decay $I_D(t)$ is expressed by the sum of two contributions, weighted by the preexponential factors B_1 and B_2. B_1 is associated with the domain where the donor is mixed with the acceptor (region 2 in Figure 3), and B_2 with the domain where the donor is without any acceptor in its vicinity (region 1 in Figure 3):

$$I_D(t) = B_1 \exp((-t/\tau) - p(t/\tau)^{1/2}) + B_2 \exp(-t/\tau) \qquad (1)$$

In eq 1, p is a time-independent parameter proportional to the local concentration of acceptor (see eq 4 below) and τ is the donor fluorescence lifetime, found equal to 46 ns in a dispersion containing only donor-labeled particles. B_1, B_2 and p are obtained by fitting eq 1 to the fluorescence decay data using a nonlinear weighted least-squares procedure. An apparent volume fraction of mixing f'_m is defined from B_1 and B_2, equal to

$$f'_m = B_1/(B_1 + B_2) \qquad (2)$$

More recently, other models were proposed to improve the analysis of the donor fluorescence intensity decay obtained using the NRET method to follow polymer interdiffusion across an interface. The sharp interfaces between donors, donors plus acceptors, and acceptors have been replaced by concentration gradients of the donors and of the acceptors. Concentration gradients have been taken into account in the more recent models proposed by Winnik and collaborators,[43,44] which lead for instance to the recovery of the acceptor or of the donor concentration profile during film annealing. Yekta et al.[45] have given a general equation of the fluorescence decay under the condition where the donors and acceptors have a nonuniform concentration profile with planar symmetry. Simulations of the donor fluorescence intensity decay were done by Dhinojwala and Torkelson.[46] Assuming a Fickian diffusion of the polymer chains through a planar interface, they showed that the fluorescence intensity decay provides excellent sensitivity for determining the polymer self-diffusion coefficient. They also proposed the use of the normalized efficiency of energy transfer, coupled with a Fickian concentration profile of the donors and acceptors, to analyze the transient fluorescence data. The final result of their calculation shows that the simplified formalism used by Winnik and collaborators underestimates the effective polymer self-diffusion coefficient.

A concentration gradient occurs inside core−shell latex particles during synthesis and can be further modified upon annealing of the core−shell latex particles.[26] In order to characterize the internal structure of our core−shell particle after synthesis, we have assumed a radial concentration profile of the donor- and acceptor-labeled polymer chains inside the composite (ideally a core−shell) particle. The distributions of the donors, $C_D(r)$, and of the acceptors, $C_A(r)$, along the radius, r, of the particle have been introduced in the classical Förster equation (3),[42] in I_0 and p, respectively:

$$I_D(r,t) = I_0 \exp((-t/\tau) - p(t/\tau)^{1/2}) \quad (3)$$

and this equation was fitted to the experimental fluorescence decay data. In eq 3, I_0 is a quantity proportional to the donor concentration $C_D(r)$, τ is the donor lifetime, and p is given by

$$p = 4\beta N R_0^{\,3} \pi^{3/2} C_A(r)/3000 = qC_A(r) \quad (4)$$

where β represents an orientation factor equal to 0.8452,[47] N is the Avogadro number, R_0 is the Förster characteristic distance equal to 23 Å in the present study, and $C_A(r)$ is the acceptor concentration.

Notice that eq 3 simply replaces eq 1 used in the previous model where a uniform distribution of the donor in regions 1 and 2 (see Figure 3) was assumed. This is the first, obvious and best improvement of the model which can be made, as also suggested elsewhere.[42−46] Equation 3 represents the fluorescence emitted by a population of donors of a given concentration $C_D(r)$, in the presence of a population of acceptors of a given concentration $C_A(r)$, situated a distance r from the center of the composite particle. Therefore the fluorescence emitted by the entire composite particle is given by

$$I_D(t) = \int_0^R C_D(r) \exp\left[-\frac{t}{\tau} - qC_A(r)\left(\frac{t}{\tau}\right)^{0.5}\right] 4\pi r^2 \, dr \quad (5)$$

where R is the particle radius. Equation 5 represents the theoretical fluorescence decay curve which should fit the experimental data; the adjustable parameters, $P(i)$, are those describing the donor and acceptor concentration profiles. Equation 5 is valid, of course, for any particle concentration. One has simply to normalize the theoretical and experimental fluorescence intensity decay curves at time $t = 0$. Another remark is that the concentration profiles must fulfill the condition that the total number of donors and acceptors in the particle stays equal to the number of donors and acceptors initially introduced in the particle during polymerization, as the adjustable parameters $P(i)$ vary. Another condition is that the total concentration of donors and acceptors in each infinitely small volume $dv(r)$ around r is constant. This last condition can be written as

$$C_A(r) = C_0 - C_D(r) \quad (6)$$

where C_0 is the donor and acceptor concentration introduced in the synthesis for the core and the shell of the particle. Thus, only the concentration profile of the donor is needed.

The time-independent adjustable parameters $P(i)$ were obtained by fitting eq 5 to the data, using a nonlinear weighted least-squares procedure based on the Levenberg−Marquardt method.[48] The modeling of the core−shell interface was done using the following concentration profiles for $C_D(r)$.

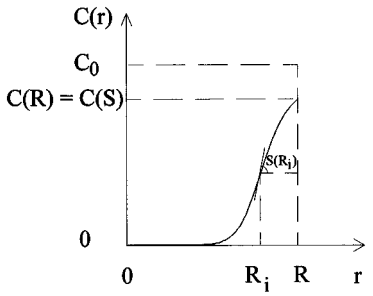

Figure 4. Schematic representation of the donor concentration profile, $C(r)$, versus r used for the best fit of eq 5 to the fluorescence decay data. At the inflection point: $r = R_i$ and the slope $= S(R_i)$.

B. Modeling of the Core−Shell Interface. The distribution of the donor from the center to the surface of the particle is assumed to present a sigmoidal shape given by

$$C_D(r) = \frac{Ar^n}{r^n + B} \quad (7)$$

where only two of the three parameters A, n, and B are independent, the third one being imposed by the fact that the number of donors introduced in the particles in the course of the synthesis must stay constant during the least-squares procedure. This means that there are only two adjustable parameters in the fitting of eq 5 to the fluorescence decay data.

It can be shown that the parameters A and B can be replaced by the parameters $C(S)$ and R_i. $C(S)$ represents the value of the donor concentration at $r = R$, i.e., at the surface of the particle; $C(S)$ is equal to or smaller than C_0. R_i is the value of r at the inflection point of the sigmoid. As can be seen in Figure 4, the parameters $C(S)$ and R_i have a straightforward physical meaning, which is not the case for the parameters A and B.

We have chosen $C(S)$ and R_i as the adjustable parameters in eq 5, n being given by

$$C_{Dt} = C_0 4\pi(R^3 - R_c^{\,3})/3 \quad (8)$$

$$C_{Dt} = \int_0^R \frac{Ar^n}{r^n + B} 4\pi r^2 \, dr \quad (9)$$

where A and B are functions of $C(S)$, R_i, and n. Equation 8 represents the number of phenanthrene groups introduced in a particle during the synthesis, whereas eq 9 is equal to the total number of phenanthrene groups calculated along the distribution profile. With $C(S)$ and R_i as adjustable parameters we had difficulties in obtaining a rapid or even a good convergence of the least-squares fit. The choice of another pair of adjustable parameters led to the same difficulties. Therefore, for each fixed R_i value, the value of $C(S)$ corresponding to the minimum value of χ^2,[48] χ_m, was determined. The variation of χ_m versus R_i went through a minimum which provided the pair R_i and $C(S)$ giving the best fit of eq 5 to the fluorescence decay data.

IV. Results and Discussion

A first indication of the degree of interpenetration between the core and the shell polymers is obtained from the analysis of the decay data with eqs 1 and 2. The volume fractions of mixing, f'_m, obtained from eq

Table 3. Values of the Fraction of Mixing, f'_{mc}, Calculated by Assuming a Sharp Interface between the Core and the Shell of the Particles, of the Fraction of Mixing, f'_m, Measured from the Fluorescence Decay Curves Using Eq 2, of the Radius, R, of the Particles Measured by AFM, of the Value of r, R_i, Corresponding to the Inflection Point of the Concentration Profile, of the Slope, $S(R_i)/C_0$, of the Concentration Profile at $r = R_i$, of f_{ts} and of $C(S)/C_0$ Obtained from Model II As Described in the Text

latex, core−shell probe	f'_m neat interface	f'_m measd	R (nm) measd	n	R_i (nm)	$S(R_i)/C_0$ (nm^{-1}) × 100	f_{ts}	$C(S)/C_0$
CS1, An−Phe	0.17	0.92	125	8.4	110	1.7	0.56	0.65
CS2, Phe−An	0.06	0.47	130	7.9	130	2.6	0.61	0.77
CS3, An−Phe	0.08	0.77	136	6.0	121	2.2	0.75	0.97
CS4, Phe−An	0.06	0.53	130	7.5	110	2.2	0.77	0.98
CS5, An−Phe	0.06	0.77	180	4.2	200	1.7	0.73	0.95
CS6, An−Phe	0.09	0.72	116	7.9	96	2.5	0.78	0.96
CS7, An−Phe	0.08	0.75	137	4.6	147	2.3	0.74	0.98
CS8, An−Phe	0.07	0.54	145	14.0	118	3.2	0.84	1
CS9, An−Phe	0.15	0.79	142	13.2	133	3.7	0.71	0.92

2, are compared in Table 3 to the fraction of mixing, f'_{mc}, calculated by assuming a sharp interface between the core and the shell of the particles, and an energy transfer between donors and acceptors taking place over a distance equal to 50 Å. One sees that the measured f'_m values are always larger than the value for perfect core−shell particles. There is therefore a diffuse interface between the core and the shell of the particles.

Results of film formation[28] show that the polymer that was expected to form the shell of the particle at the end of the synthesis was indeed located at the periphery of the particles. This gives the sign of the concentration gradient of the phenanthrene-labeled polymer chains to use in the model. The concentration gradient is decreasing from the surface to the center of the particle for latexes CS1, CS3, and CS5 to CS9, and increasing for latexes CS2 and CS4. One must note that this gradient might not simply result from a Fickian type of diffusion of the polymer chains inside the particles. It occurs inside the particles during the synthesis of the shell. At that time the temperature of the core is 80 °C (polymerization temperature), which is much above its glass transition temperature (34 °C). Thus, some monomers, oligomers, or small molecular weight growing polymer chains can probably migrate during synthesis from the periphery to the center of the particles. This process of diffusion involves different diffusion coefficients, and there is no reason that a Fickian process of diffusion, involving a unique diffusion coefficient, would provide a model representative of this gradient. In the absence of a good theoretical model, the simple model described above has been used.

A. Internal Structure. Parts a and b of Figure 5 show the best fits of eq 5 with the model to the fluorescence decay data for CS3 and CS4, respectively. Between CS3 and CS4, the labeling of the core and of the shell are inverted (see Table 2). It is worth noting that the fits are good in both cases (Figure 5).

Some parameters characterizing the shell polymer concentration profiles are given in Table 3. $S(R_i)$ is the slope of the concentration profile at the inflexion point, R_i. It increases as the stiffness of the shell polymer concentration profile increases and is infinite for a perfect core−shell particle. f_{ts} is the fraction of donor comprising in the theoretical shell thickness of the particle. It was obtained by integration of the donor concentration profile inside the theoretical shell thickness, divided by the total number of donors in the whole particle. This parameter directly indicates to which extent the synthesis of the core−shell particles was successful. The values of $C(S)$ have been normalized to C_0. A value of 1 for the ratio $C(S)/C_0$ indicates that the phenanthrene concentration at the surface of the particle is equal to the concentration, C_0, for a perfect core−shell particle. In the case of CS2 and CS4 the parameters in Table 3 characterize the anthracene profile and not the phenanthrene profile.

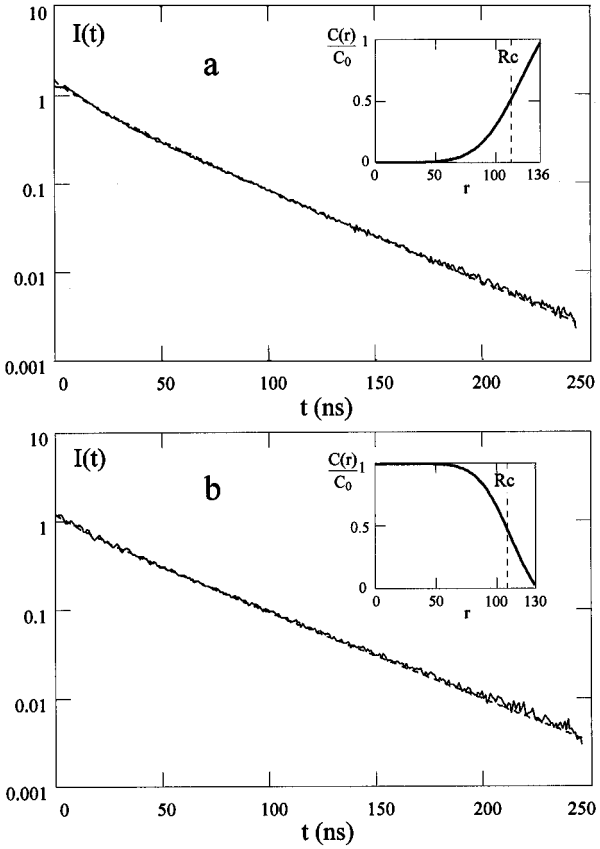

Figure 5. Best fit (dashed line) of eq 5 to the fluorescence decay data obtained with the model for the core−shell particles CS3 (a) and CS4 (b) in dispersion. The insets represent the donor concentration profile found for the best fit.

The most interesting parameter is f_{ts}. Despite of the diffuse interface between the core and the shell of the particles, the values of f_{ts} indicate that more than 70% of the polymer which should form the shell of the particles is comprised in the theoretical shell volume for CS3 and CS4, but only between 55% and 62% for CS1 and CS2, due to their lower shell thickness. f_{ts} would probably decrease with a further decrease of the shell thickness, since it becomes more and more difficult to keep the polymer for the shell in a narrow volume around the core of the particle as the shell becomes thinner. The ratio $C(S)/C_0$ also decreases as one goes from CS3 and CS4 to CS1 and CS2. Here again the decrease is due to the lower shell thickness of the CS1

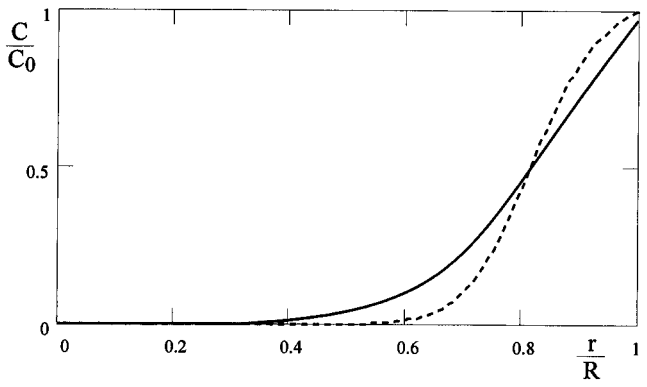

Figure 6. Comparison of the donor concentration profiles obtained for CS3 (full line) and CS8 (dashed line) from the best fit of eq 5 to the fluorescence decay data.

and CS2 particles. Note that the latexes CS3 and CS4, whose labelings are complementary, give very close values for the parameters $S(R_i)/C_0$, f_{ts} and $C(S)/C_0$. Note also that the values of R_i are very close to the values of the theoretical core radius R_c given in Table 2. This brings credibility to the model.

B. Optimization of the Core−Shell Interface. The modifications to the synthesis of the core−shell particles CS1 to CS4 described in Latex Synthesis were made with the goal of sharpening the interface between the core and the shell of the particles. Following the synthesis undertaken by others,[49] we reduced the hydrophilic character of the core polymer by using AIBN as initiator for the polymerization of butyl methacrylate, rather than KPS which give rise to ionic $-SO_4-$ terminal groups, which can promote the contact of the core PBMA with the water phase. This led to particles CS5. We also tried to reduce penetration of the shell polymer into the core of the particle by cross-linking the core with 5 wt % allyl methacrylate. This led to particles CS6. Finally, in the synthesis of particles CS7, CS8, and CS9 we tried to increase the incompatibility between the core and the shell. This was done by synthesizing in latex CS7 a purely fluorinated shell using TFEM as monomer, and by adding styrene in the synthesis of the core of the particles CS8 and CS9. The main characteristics of the particles CS5 to CS9 are given in Table 2, whereas the results of the best fits obtained with the model are reported in Table 3.

Particles Having a Core/Shell Weight Ratio Equal to 56/44 (CS3 to CS8). Between CS3 and CS5 there is not much effect on the donor concentration profile, as shown in Table 3. Very close values were found for $S(R_i)/C_0$, f_{ts}, and $C(S)/C_0$. The only difference is the increase of the particle size when AIBN is used. Table 3 also indicates that there is no modification of the donor concentration profiles between the CS3 and the CS6 or CS7 particles. In contrast to these results a large difference in the value of the parameters is observed between the CS3 and the CS8, i.e., as one introduces styrene in the core polymer: $S(R_i)/C_0$ and f_{ts} increase which indicates that the concentration profile becomes sharper, and $C(S)/C_0$ reaches the value of 1, which indicates that the particle surface is fully covered by the shell polymer. These results are clearly illustrated in Figure 6 where the concentration profiles obtained with CS3 and CS8 are shown: CS8 presents a stiffer concentration profile than CS3.

Particles Having a Core/Shell Weight Ratio Equal to 74/26 (CS1 and CS9). The introduction of styrene in the core polymer of particles having a theoretical core/shell weight ratio equal to 74/26 led to the same conclusion as above. Indeed, Table 3 shows that $S(R_i)/C_0$, f_{ts}, and $C(S)/C_0$ increase between CS1 and CS9. Thus, a narrower interface between the core and the shell is found for the particle CS9 containing styrene in the core.

The above results indicate that there is less diffusion of the shell monomers, oligomers, or polymers from the surface to the center of the particle during synthesis of the latexes CS8 and CS9 than for any other latex particles synthesized in this work. This comes from a greater thermodynamic incompatibility between the core and the shell of the particle upon addition of styrene in the core during the synthesis.

V. Conclusion

The aim of this work was to obtain information on the internal structure of core−shell latex particles from the fluorescence NRET method which can be applied in principle to any type of polymer, which is not the case for other techniques like TEM for instance. The present study has been carried out on latex particles in dispersion. The polymers forming the core and the shell of the particles were labeled either with the acceptor in the core and the donor in the shell or reciprocally. Using a simple model for the concentration profile of the shell polymer in the latex particles, a quantification of the diffuse interface between the core and the shell of the particles was possible. Good fits of the theoretical fluorescence decay curve to the experimental decays were found. Labeling of the core or of the shell of the particles with the donor gave the same concentration profiles. We have tried to improve the core−shell character of the particles by introducing several modifications to the synthesis. We avoided end charges on the core polymer by using AIBN as initiator in the core synthesis, we cross-linked the core with allyl methacrylate to hinder the penetration of the shell polymer in the core of the particle, and we tried to make the shell-polymer less compatible with the core polymer by using pure fluorinated monomer for the synthesis of the shell. None of these modifications had any effect on the distribution of the core and shell polymers inside the particle. However, the core−shell character of our particles was substantially improved by introducing styrene during the synthesis of the core polymer. This work also shows, on a more general basis, that the fluorescence NRET method can be used to obtain information on the internal structure of the core−shell latex particles and is suitable for testing various synthesis processes for the design of tailored core−shell particles.

Acknowledgment. The authors thank Elías Pérez for fruitful discussions, and P.M. thanks Elf Atochem for its financial support and its interest in this work.

References and Notes

(1) Sundberg, D. C.; Casassa, A. P.; Pantazopoulos, J.; Muscato, M. R.; Kronberg, B.; Berg, J. *J. Appl. Polym. Sci.* **1990**, *41*, 1425. Sundberg, E. J.; Sundberg, D. C. *J. Appl. Polym. Sci.* **1993**, *47*, 1277.
(2) Grancio, M. R.; Williams, D. J. *J. Polym. Sci., Polym. Chem. Ed.* **1970**, *8*, 2617.
(3) Keusch, P.; Williams, D. J. *J. Polym. Sci., Polym. Chem. Ed.* **1973**, *11*, 143.
(4) Kanig, G.; Neff, H. *Colloid. Polym. Sci.* **1975**, *253*, 29.
(5) Vandezande, G. A.; Rudin, A. *J. Coatings Technol.* **1994**, *66*, 99.

(6) Okubo, M.; Katsuta, Y.; Matsumoto, T. *J. Polym. Sci., Polym. Lett. Ed.* **1982**, *20*, 45.
(7) Min, T. I.; Klein, A.; El-Aasser, M. S.; Vanderhoff, J. W. *J. Polym. Sci., Polym. Chem. Ed.* **1983**, *21*, 2845.
(8) Chen, Y.-C.; Dimonie, V.; El-Aasser, M. S. *Macromolecules* **1991**, *24*, 3779. Chen, Y.-C.; Dimonie, V. L.; Shaffer, O. L.; El-Aasser, M. S. *Polym. Int.* **1993**, *30*, 185.
(9) Jönsson, J.-E.; Hassander, H.; Törnell B. *Macromolecules* **1994**, *27*, 1932.
(10) He, W.; Tong, J.; Wang, M.; Pan, C.; Zhu, Q. *J. Appl. Polym. Sci.* **1995**, *55*, 667.
(11) Hergeth, W.-H.; Bittrich, H.-J.; Eichhorn, F.; Schlenker, S.; Schmutzler, K.; Steinau, U.-J. *Polymer* **1989**, *60*, 1913.
(12) Kamei, S.; Okubo, M.; Masumoto, T. *J. Polym. Sci., Polym. Chem. Ed.* **1986**, *24*, 3109.
(13) O'Reilly, J. M.; Melpolder, S. M.; Fischer, L. W.; Wignall, G. D.; Ramakrishnan, V. *Polym. Prepr. (Am. Chem. Soc., Div. Polym. Chem.)* **1983**, *24* (2), 407. Fischer, L. W.; Melpolder, S. M.; O'Reilly, J. M.; Ramakrishnan, V.; Wignall G. D. *J. Colloid Interface Sci.* **1988**, *123*, 24.
(14) Wai, M. P.; Gelman, R. A.; Fatica, M. G.; Hoerl, R. H.; Wignall, G. D. *Polymer* **1987**, *28*, 918.
(15) Grunder, R.; Urban, G.; Ballauff, M. *Colloid Polym. Sci.* **1993**, *271*, 563.
(16) Dingenouts, N.; Ballauff, M. *Acta Polym.* **1993**, *44*, 178.
(17) Ballauff, M. *Macromol. Symp.* **1994**, *87*, 93.
(18) Tembou Nzudie, D.; Delmotte, L.; Riess, G. *Makromol. Chem., Rapid Commun.* **1991**, *12*, 251; *Macromol. Chem. Phys.* **1994**, *195*, 2723.
(19) Dobler, F.; Pith, T.; Holl, Y.; Lambla, M. *J. Appl. Polym. Sci.* **1992**, *44*, 1075.
(20) Muroi, S.; Hashimoto, H.; Hosoi, K. *J. Polym. Sci., Polym. Chem. Ed.* **1984**, *22*, 1365.
(21) Misra, S. C.; Pichot, C.; El-Aasser, M. S.; Vanderhoff, J. W. *J. Polym. Sci., Polym. Lett. Ed.* **1979**, *17*, 567.
(22) Misra, S. C.; Pichot, C.; El-Aasser, M. S.; Vanderhoff, J. W. *J. Polym. Sci., Polym. Chem. Ed.* **1983**, *21*, 2383.
(23) Cavaillé, J. Y.; Jourdan, C.; Kong, X. Y.; Perez, J.; Pichot, C.; Guillot, J. *Polymer* **1988**, *27*, 693.
(24) Sommer, F.; Tran Min Duc; Pirri, R.; Meunier, G.; Quet, C. *Langmuir* **1995**, *11*, 440.
(25) Winnik, M. A.; Xu, H.; Satguru, R. *Makromol. Chem., Macromol. Symp.* **1993**, *70/71*, 107.
(26) Pérez, E.; Lang, J. *Langmuir* **1996**, *12*, 3180.
(27) Zhao, C.-L.; Wang, Y.; Hruska, Z.; Winnik, M. A. *Macromolecules* **1990**, *23*, 4082.
(28) Marion, P.; Beinert, G.; Juhué, D.; Lang, J. To appear in *J. Appl. Polym. Sci.*
(29) Pfeffer, G.; Lami, H.; Laustriat, G.; Coche, A. *C. R.. Hebd. Séances Acad. Sci.* **1963**, *257*, 434.
(30) Kim, H.-B.; Wang, Y.; Winnik, M. A. *Polymer* **1994**, *35*, 1779.
(31) Pekcan, Ö.; Winnik, M. A.; Croucher, M. D. *Macromolecules* **1990**, *23*, 2673.
(32) Wang, Y.; Zhao, C.-L.; Winnik, M. A. *J. Chem. Phys.* **1991**, *95*, 2143.
(33) Wang, Y.; Winnik, M. A. *J. Coat. Technol.* **1992**, *64*, 51.
(34) Wang, Y.; Winnik, M. A. *Macromolecules* **1993**, *26*, 3147.
(35) Wang, Y.; Winnik, M. A. *J. Phys. Chem.* **1993**, *97*, 2507.
(36) Wang, Y.; Winnik, M. A. *Macromolecules* **1990**, *23*, 4731.
(37) Juhué, D.; Wang, Y.; Winnik, M. A. *Makromol. Chem., Rapid Commun.* **1993**, *14*, 345.
(38) Boczar, E. M.; Dionne, B. C.; Fu, Z.; Kirk, A. B.; Lesko, P. M.; Koller, A. D. *Macromolecules* **1993**, *26*, 5772.
(39) Juhué, D.; Lang, J. *Macromolecules* **1994**, *27*, 695.
(40) Juhué, D.; Lang, J. *Double Liaison-Physique et Chimie des Peintures et Adhésifs* **1994**, *464−465*, 3.
(41) Juhué, D.; Lang, J. *Macromolecules* **1995**, *28*, 1306.
(42) Förster, Th. *Ann. Phys. (Leipzig)* **1948**, *2*, 55; *Discuss. Faraday Soc.* **1959**, *27*, 7.
(43) Liu, Y. S.; Li, L.; Ni, S.; Winnik, M. A. *Chem Phys.* **1993**, *177*, 579.
(44) Liu,Y. S.; Feng, J.; Winnik, M. A. *J. Chem. Phys.* **1994**, *101*, 9096.
(45) Yekta, A.; Duhamel, J.; Winnik, M. A. *Chem. Phys. Lett.* **1995**, *235*, 119.
(46) Dhinojwala, A.; Torkelson, J. M. *Macromolecules* **1994**, *27*, 4817.
(47) Baumann, J.; Fayer, M. D. *J. Chem. Phys.* **1986**, *85*, 4087.
(48) Press, W. H.; Teukolsky, S. A.; Vetterling, W. T.; Flannery, B. P. *Numerical Recipes in Fortran: The Art of Scientific Computing*, 2nd ed.; Cambridge University Press: Cambridge, U.K., 1992.
(49) Cho, I.; Lee, K.-W. *J. Appl. Polym. Sci.* **1985**, *30*, 1903.

MA960392N